Electronic Supplementary Material (ESI) for Chemical Communications.

Electronic Supplementary Information to:

Aggregation- and Cyclization-induced Chirality Amplification of Optically Active Fluorescent Polyurethane in the Ground and Exited States

Zhiyi Song,[a] Hiroyasu Sato,[b] Adriana Pietropaolo,[c] Qingyu Wang,[a] Shuhei Shimada,[d] Heshuang Dai,[a] Yoshitane Imai,[e] Hayato Toda,[e] Takunori Harada,[f] Yukatsu Shichibu,[g] Katsuaki Konishi,[g] Masayoshi Bando,[a] Naofumi Naga,[h] and Tamaki Nakano*[a,i]

[a] Institute for Catalysis (ICAT) and Graduate School of Chemical Sciences and Engineering, Hokkaido University, N21W10, Kita-ku, Sapporo 001-0021 (Japan)
[b] Rigaku Corporation 4-14-4, Sendagaya, Shibuya-Ku, Tokyo 151-0051 (Japan)
[c] Dipartimento di Scienze della Salute, Università di Catanzaro, Catanzaro (Italy)
[d] Technical Division, Institute for Catalysis, Hokkaido University, N21W10, Kita-ku, Sapporo 001-0021, Japan
[e]Graduate School of Science and Engineering, Kindai University, 3-4-1 Kowakae, Higashiosaka City, Osaka 577-8502 (Japan)
[f] Department of Integrated Science and Technology, Faculty of Science and Technology Oita University, Dannoharu, 700, Oita City 870-1192 (Japan)
[g] Faculty of Environmental Earth Science, Hokkaido University, N10, W5, Kita-ku, Sapporo 060-0810 (Japan)
[h] Department of Applied Chemistry, Shibaura Institute of Technology, College of Engineering, 3-7-5 Toyosu, Koto-ku, Tokyo 135-8548, Japan
[i] Integrated Research Consortium on Chemical Sciences (IRCCS), Institute for Catalysis, Hokkaido University, N21W10, Kita-ku, Sapporo 001-0021 (Japan)

*Correspondence should be addressed to Tamaki Nakano
(E-mail: tamaki.nakano@cat.hokudai.ac.jp)

Table of Contents

Experimental

Materials. Triphosgene (TCI), 2,7-diaminofluorene dihydrochloride (TCI), triethylamine (Aldrich), and (*R*)-(+)- and (*S*)-(-)- 2,2'-dihydroxy-1,1'-binaphthyl (Kanto Chemical), were used as purchased.

General instrumentation. ^{1}H NMR spectra in solution were recorded on a JEOL JNM-ECX400 spectrometer (400 MHz for ^{1}H measurement) and a JEOL JNM-ECA600 spectrometer (600 MHz for ^{1}H measurement). SEC measurements were carried out using a chromatographic system consisting of a Hitachi L-7100 chromatographic pump, a Hitachi L-7420 UV detector (254 nm), and a Hitachi L-7490 RI detector equipped with series (eluent THF, flow rate 1.0 mL/min). Preparative SEC analyses were carried out using a JAI LC-9201 chromatograph with an S-3740 detector equipped with JAIGEL-1H and 2H columns connected in series (eluent $CHCl_3$, flow rate 3.5 mL/min), a JAI LC-9201 chromatograph with a UV-50 and an RI-50 RI detectors equipped with JAIGEL-1H and 2H columns connected in series (eluent $CHCl_3$, flow rate 3.8 mL/min), an Laboace LC-5060 chromatograph with a 4ch800LA and a 700LA detectors equipped with JAIGEL-1RH, 2RH, and 3RH connected in series (eluent $CHCl_3$, flow rate 10.0 mL/min). UV-vis absorption spectra were measured with a JASCO V-570 spectrophotometers. Emission spectra were taken on a JASCO FP-8500 fluorescence spectrophotometer. IR spectra were recorded on a JASCO FT/IR-6100 spectrometer using KBr pellet samples. Circular dichroism (CD) spectra were taken with a JASCO-820 spectrometer. Differential scanning calorimetry (DSC) and thermal gravity analysis (TGA) were taken on Rigaku Thermo Plus DSC8230 and TG8120 analyzer at a heating rate of 10 K/min in nitrogen atmosphere. CPL spectra were measured with a JASCO-300 spectrometer and with an apparatus based on a photo elastic modulator and a photomultiplier assembled according the literature[1] with modifications. FD mass spectrometry was performed on a JEOL JMS-T100GCv apparatus. DLS analysis was conducted using an NICOMP-380 particle sizer. TEM images were obtained on a JEM-2100F microscope at 200 kV using a micro grid. XRD profiles were measured using a Rigaku MiniFlex600-C diffractometer.

2,7-Diisocyananatofluorene (27DIF).[2] 2,7-Diaminofiluorene dihydrochloride (1.0 g, 3.7 mmol) was suspended in 80 mL CH_2Cl_2. After bubbled with N_2 for 15 mins, the mixture was added with triethylamine (1.11 mL, 8.0 mmol) at 23 °C and stirred for 1 h. To a clear solution was slowly added a 20-mL CH_2Cl_2 solution of triphosgene (1.0 g, 3.3 mmol) at 23 °C in a 1-h duration. The reaction mixture was then refluxed for 2 h. After cooling, the reaction mixture was washed with 100 mL water twice and dried on $MgSO_4$. Evaporation of the solvent gave 0.9 g of light-yellow solid (yield 98%). ^1H NMR (600 MHz, 298 K, $CDCl_3$) δ/ppm: 7.65 (2 H, d, $J = 8.1$ Hz), 7.26 (2 H, s), 7.10 (2 H, d, $J = 8.1$ Hz), 3.85 (2 H, s); ^{13}C NMR (150 MHz, 298 K, $CDCl_3$) δ/ppm: 144.6, 138.6, 132.0, 124.8, 123.8, 121.6, 120.6, 36.7; IR (KBr) υ/cm^{-1}: 3406, 2267, 1653, 1602, 1523, 1438, 1392, 1232, 1107, 827, 566.

Polymerization. The polymerization procedure corresponding to run 6 in Table S1 is describe here as the most typical example. 27DIF (0.124 g, 0.5 mmol) and (*R*)-(+)-2,2'-dihydroxy-1,1'-binaphthyl (0.143 g, 0.5 mmol) were dissolved in 3.1 mL of acetone under N_2 atmosphere, and triethylamine (0.152 g, 1.5 mmol) were injected to initiate the polymerization. The reaction mixture was allowed to stand at 20 °C for 24 h. Finally, the reaction was terminated by the addition of methanol (0.5 mL) for 10 mins. The products were reprecipitated in methanol, collected with a centrifuge (10,000 rpm, 10 min) and dried under vacuum. The crude products were further purified by preparative SEC to give polyurethane (0.136 g, 51% yield) and cyclic dimer (0.077 g, 29% yield).

Polyurethane: ^1H NMR (600 MHz, 298 K, $CDCl_3$) δ/ppm: 10.02-10.08 (m, N-H), 7.98-7.08 (m, Ar-H), 3.89-3.21 (m, alkyl-H); IR (KBr) υ/cm^{-1}: 3399, 1737, 1590, 1537, 1470, 1353, 1187, 1072, 1018, 815, 749.

Cyclic dimer: ^1H NMR (600 MHz, 298 K, DMSO-d_6) δ/ppm: 9.62 (4 H, s), 8.13 (4 H, d, $J =$ 6.0 Hz), 8.08 (4 H, d, $J = 12.0$ Hz), 7.61 (4 H, d, $J = 6.0$ Hz), 7.56 (4 H, d, $J = 6.0$ Hz), 7.51 (4 H, t, $J = 6.0$ Hz), 7.35(4 H, t, $J = 6.0$ Hz), 7.16 (4 H, s), 7.01(4 H, d, $J = 6.0$ Hz), 6.94 (4 H, d, $J = 12.0$ Hz), 3.24 (4 H, s); ^{13}C NMR (150 MHz, 298 K, DMSO-d_6) δ/ppm: 152.0, 146.9, 142.7, 136.4, 136.3, 133.0, 130.7, 128.8, 128.0, 126.5, 125.2, 123.0, 122.3, 120.3, 118.7, 118.4, 36.2; IR (KBr) υ/cm^{-1}: 3404, 1750, 1590, 1535, 1470, 1210, 1076, 1016, 823, 748; HR-MS (ESI) calcd. for $C_{70}H_{44}O_9N_4Na$: 1091.30514; found: 1091.30805.

Crystal structure analysis. Crystal data were collected on a Rigaku XtaLAB Synergy-R diffractometer with multi-layer mirror optics Cu Kα radiation (λ = 1.54184 Å) at 100.01 K, and all calculations were performed using CrysAlis^{Pro} (Rigaku Oxford Diffraction, 2021). Empirical absorption corrections were applied using spherical harmonics, implemented in SCALE3 ABSPACK scaling algorithm. The crystal structures were solved by direct methods

(SHELXT 2018/2)[3] and refined by full-matrix least-squares methods on F^2 values (SHELXL 2018/3),[4] interfaced through the program OLEX2. Anisotropic temperature factors were applied to all non-hydrogen atoms. The hydrogen atoms were put at calculated positions, and refined applying riding models. Crystal data for the cyclic dimer·6THF: $C_{70}H_{44}N_4O_8,6(C_4H_8O)$; M = 1501.71, crystal dimensions 0.193 × 0.043 × 0.035 mm^3; orthorhombic; space group $P2_12_12_1$ (no. 19); a = 10.27320(10) Å, b = 26.8858(3) Å, c = 28.5990(3) Å; V = 7899.14(14) Å^3; Z = 4; ρ_{calcd} = 1.263 gcm^{-3}; μ = 0.682 mm^{-1}; 2θmax = 146.64°; reflections collected: 83273, independent reflections: 16842 (R_{int} = 0.0622), R1($F^2>2\sigma$) = 0.0726, wR2(F^2) = 0.2313; final difference map within +0.459 and -0.286 eÅ^3, Flack Parameter χ = 0.11 (8). CCDC-2106634 ((S)-BINOL-27DIF cyclic dimer) contains the supplementary crystallographic data for this paper. These data can be obtained free of charge from The Cambridge Crystallographic Data Centre via www.ccdc.cam.ac.uk/data_request/cif.

Computational method. Wave-form analysis of SEC curves for determination of the contents of polymers and dimers were performed using Origin 2018 software package (Origin Lab). Molecular mechanics structure optimization was run using the COMPASS[5] force field implemented in the Discover module of the Material Studio 4.2 (Accelrys) software package with the Fletcher-Reeves[6] conjugate gradient algorithm until the RMS residue went below 0.01 kcal/mol/Å. Molecular dynamic simulation was performed under a constant NVT condition in which the numbers of atoms, volume, and thermodynamic temperature were held constant. Berendsen's thermocouple[7] was used for coupling to a thermal bath. The step time was 1 fs and the decay constant was 0.1 ps. Conformations obtained through MD simulation were saved in trajectory files at every 5 or 10 ps and were optimized by MM simulation.

Electronic CD Spectra calculations. The initial coordinates of a 3-mer of poly(R-BINOL-alt-27DIF) in anti and syn conformations were obtained through MD simulations at 300 K. From those coordinates, initial geometry optimizations were run at the HF/6-31G* level of theory, followed by 50 steps of ab-initio molecular dynamics in the framework of Atom Centered Density Matrix Propagation[8,9] at 300 K at the same level of theory within Gaussian 16 package.[10]

The intrinsic rotational strengths were calculated considering 50 singlet excited states of the syn and anti 3-mer conformations at the ZINDO level.[11,12] Rotatory strengths are reported in the usual c.g.s. units of 10^{-40} esu.cm.erg/Gauss. The rotational strength R_i associated with an electronic transition 0→ i at frequency ν_i is estimated from quantum-mechanics from the dipole-length formalism as follows[13]

$$R_i(length) = \mathrm{Im}(\boldsymbol{\mu}_{0i} \bullet \mathbf{m}_{0i}) \qquad 1)$$

where $\boldsymbol{\mu}_{0i}$ is the electric dipole transition moment and $\mathbf{m}_{0i}$ the magnetic dipole transition moment. The calculations of the ECD spectra at a given wavelength, λ, were done assuming Gaussian bands with 800 cm^{-1} full width at half-height (from 200 nm to 500 nm) for all transitions centered in each excitation wavelength. The ECD spectra were blue-shifted of 30 nm with respect to those experimentally recorded. A factor of 2.278 was applied during the conversion of rotational strengths and Δε values, as reported in Refs.[14,15]

The calculations of electronic UV spectra were done in the same way, with full width at half-height of 1200 cm^{-1} and assuming the factor 2.8710^{10} accounting for the conversion between oscillator strengths and the molar extinction coefficients.[16]

TD-DFT simulations were run at the wB97XD/6-31G* level of theory[17] in the first excited state of the cyclic dimer, followed by charge calculations according to the Merz-Singh-Kollman scheme[18] and dipole moment calculations in the ground (previously optimized at the wB97XD/6-31G* level of theory) and in the first excited state.

Table S1. Synthesis of Poly((*R*)-BINOL-*alt*-27DIF) by polyaddition under various conditions using Et_3N as catalyst under N_2[a]

Run[a]	**[27DIF]**	[**BINOL**]	Solvents	Temp.	Conv. (%)[b]	Cyclic dimer Yield (%)[c]	Polymer Yield (%)	Polymer M_n[d]	Polymer M_w/M_n[d]
1	0.16	0.16	Ethyl acetate	23 °C	91	26	62	2060	2.21
2	0.032	0.032	Ethyl acetate	23 °C	84	51	33	1180	2.82
3	0.8	0.8	Ethyl acetate	23 °C	93	33	54	2740	2.04
4	0.16	0.16	Ethyl acetate	0 °C	96	29	67	2360	1.98
5	0.16	0.16	Ethyl acetate	50 °C	73	24	48	1160	1.27
6	0.16	0.16	Acetone	23 °C	86	29	51	2170	1.83
7	0.032	0.032	Acetone	23 °C	95	64	10	2570	1.52
8	0.8	0.8	Acetone	23 °C	94	23	71	2080	1.52
9	0.16	0.16	Acetone	0 °C	97	20	76	2820	2.72
10	0.16	0.16	Acetone	50 °C	89	43	45	1330	1.33
11	0.16	0.16	THF	23 °C	97	47	49	1530	1.23
12	0.032	0.032	THF	23 °C	73	51	22	1370	1.18
13	0.8	0.8	THF	23 °C	72	14	68	1570	1.25
14	0.16	0.16	THF	0 °C	78	36	42	1700	1.28
15	0.16	0.16	THF	50 °C	85	38	47	1320	1.06
16	0.16	0.16	CS_2	23 °C	96	16	80	1970	1.53
17	0.16	0.16	CH_3CN	23 °C	98	11	87	2390	2.66

[a] Conditions: BINOL = 28.6 mg (0.1 mmol) (runs 2-5, 7-10, 12-17), 286.3 mg (1.0 mmol) (runs 1, 6, 11); 27DIF = 24.8 mg (0.1 mmol) (runs 2-5, 7-10, 12-17), 248.4 mg (1.0 mmol) (runs 1, 6, 11); [Et_3N] = 0.71M, reaction time = 24 h. [b] Determined by ^1H NMR spectra of crude mixture. [c] Estimated by SEC with UV detection at 254 nm. [d] Determined by SEC using polystyrene standard.

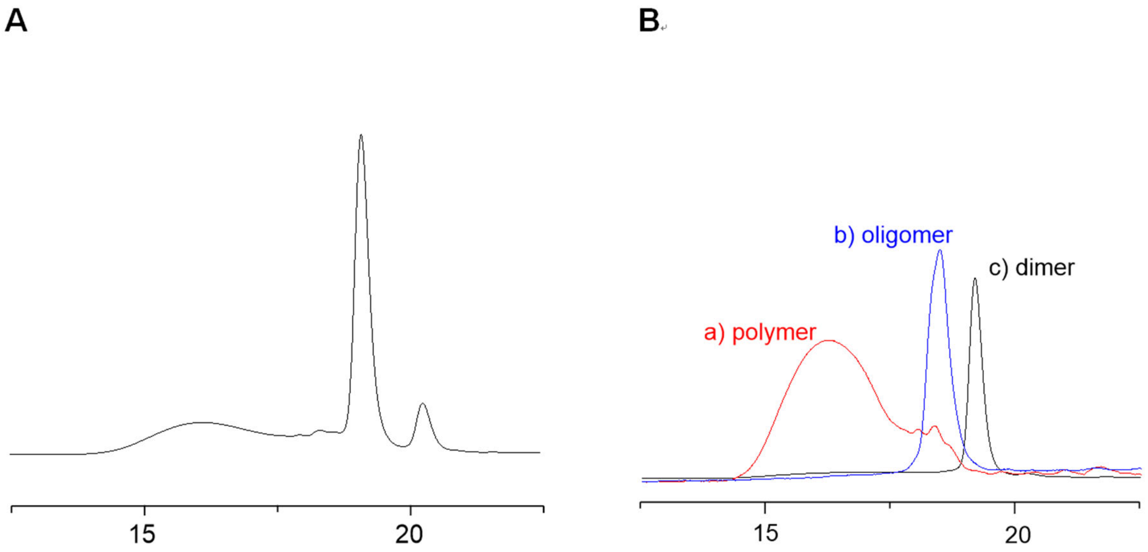

Fig. S1. SEC profiles of the entire products from Run 6 in Table S1 (A) and those of the separated linear polymers of *M*n 4100 (a) and *M*n 1100 (b) and the cyclic dimer (c) separated from the products obtained using preparative SEC (B).

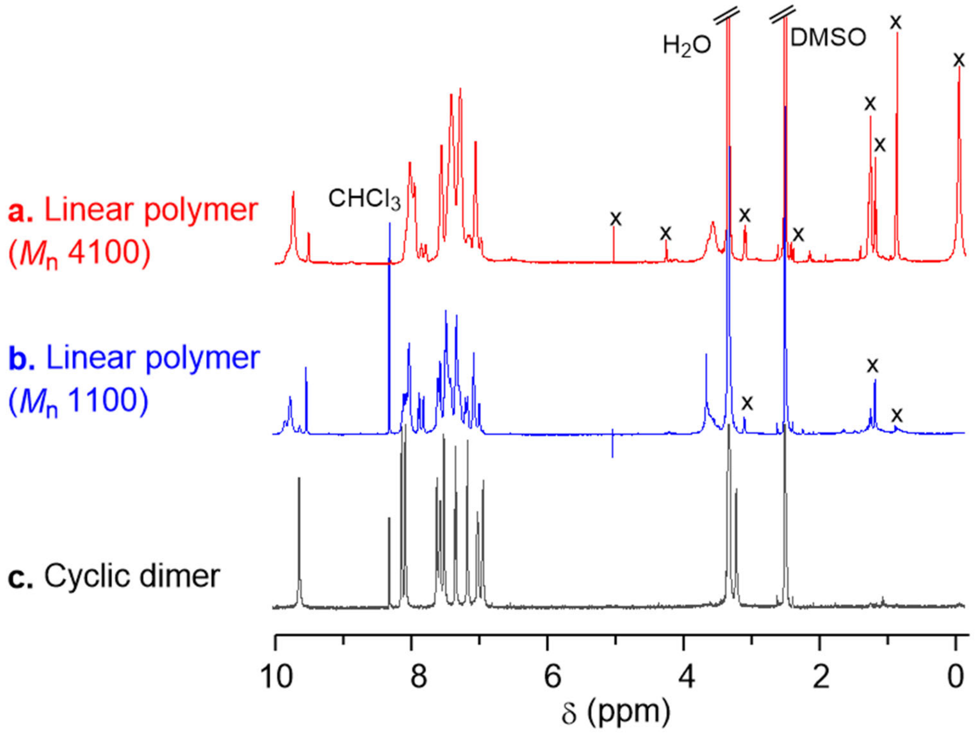

Fig. S2. ^{1}H NMR spectra of polymers of *M*n 4100 (a) and 1100 (b) and the cyclic dimer (c) from run 6 in Table S1. [400 MHz, DMSO-d_6 (a) and $CDCl_3$ (b), r.t.]

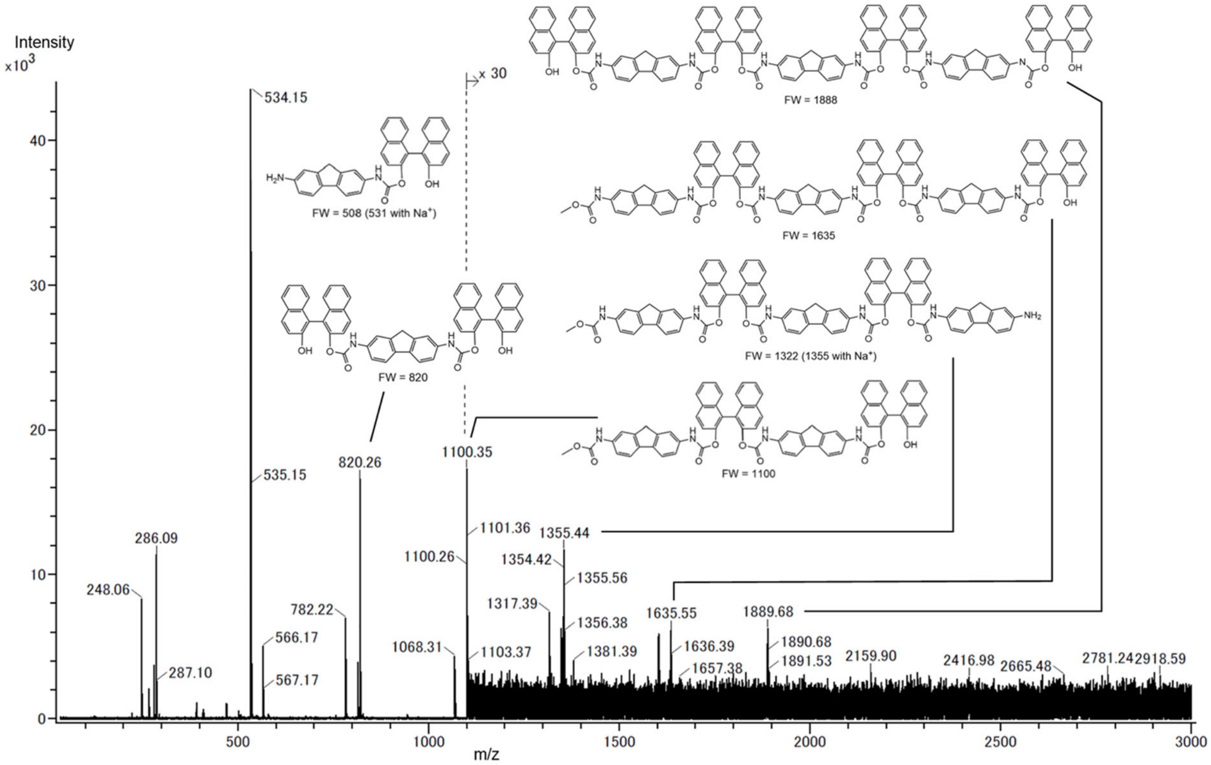

Fig. S3. FD mass spectrum of linear polymer of M_n 1100.

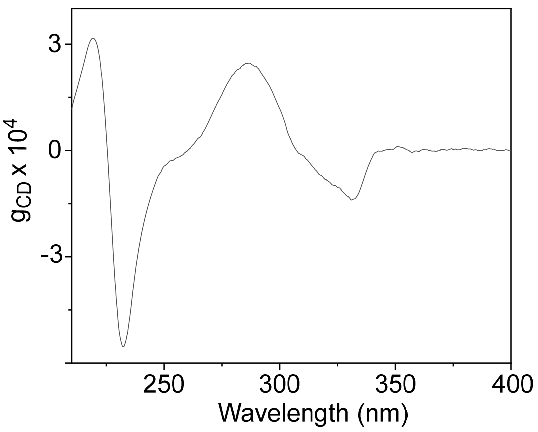

Fig. S4. g_{CD} spectrum of poly((*R*)-BINOL-*alt*-27DIF)s of M_n's 4100 corresponding to Fig. 1 A (**a**) in the main manuscript. [THF, 1.0 x 10^{-4} M, 1-mm cell]

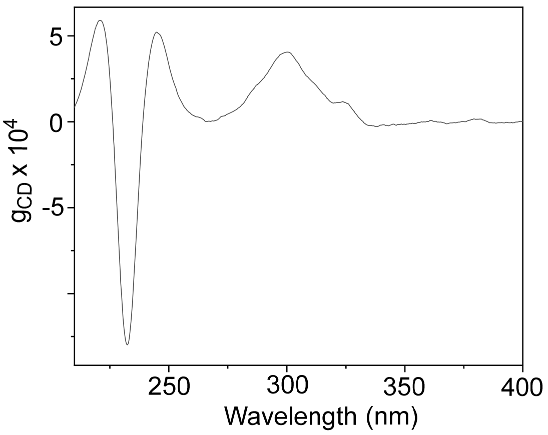

Fig. S5. g_{CD} spectrum of (*R*)-BINOL-27DIF cyclic dimer corresponding to Fig. 3 B (**a**) in the main manuscript. [THF, 1.1 x 10^{-4} M, 1-mm cell]

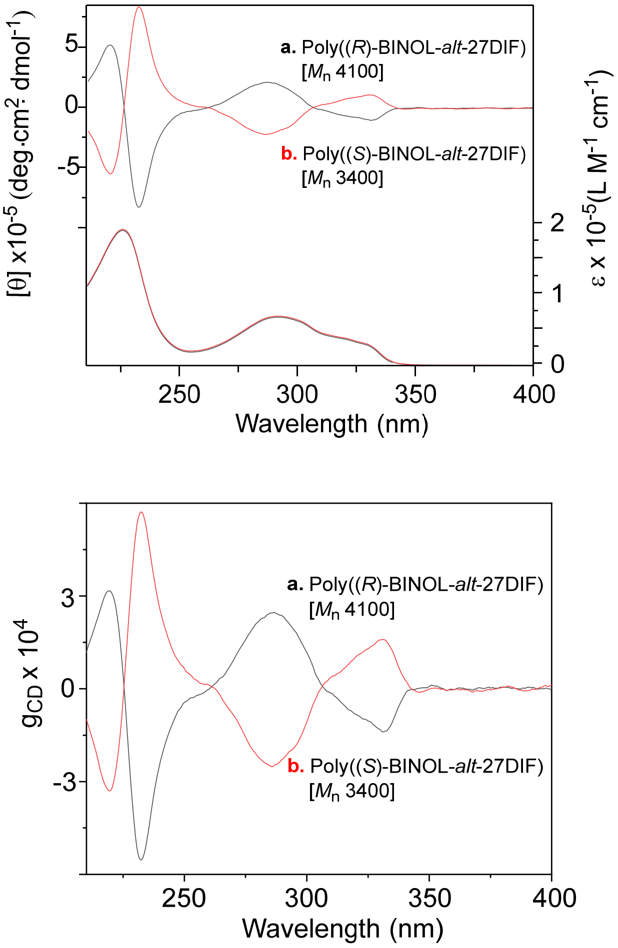

Fig. S6. CD-UV spectra of linear polymers using (*R*)-BINOL (a) and (*S*)-BINOL (b) [top] and corresponding g_{CD} spectra [bottom].

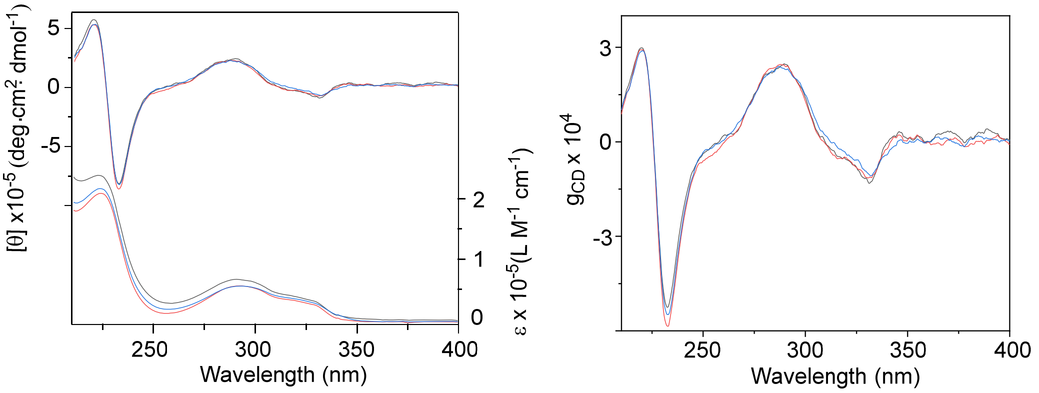

Fig. S7. CD-UV spectra of linear polymers obtained at 0 ºC (run 4 in Table S1) (a), 23 ºC (run 1 in Table S1) (b), and 50 ºC (run 5 in Table S1) (c) in ethyl acetate [left] and corresponding g_{CD} spectra [right]. [θ] in A is based on the molarity of the residue composed of a BINOL unit and a 27DIF unit.

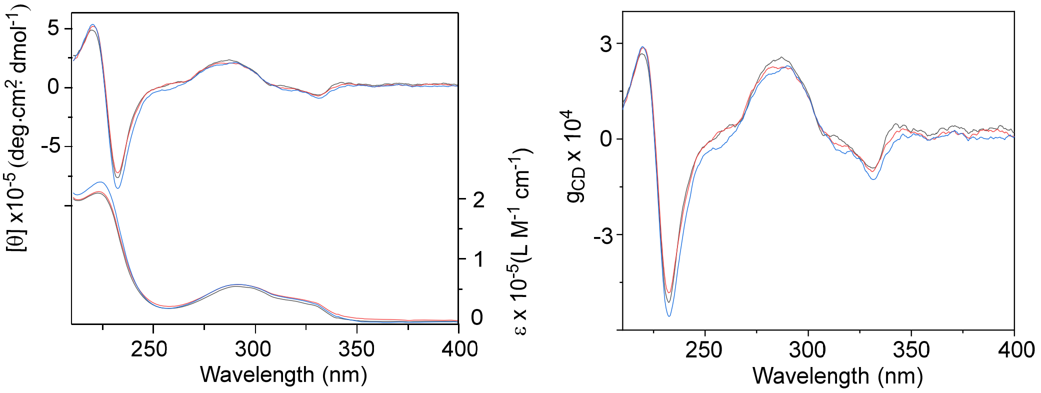

Fig. S8. CD-UV spectra of linear polymers obtained at 0 ºC (run 9 in Table S1) (a), 23 ºC (run 6 in Table S1) (b), and 50 ºC (run 10 in Table S1) (c) in acetone [left] and corresponding g_{CD} spectra [right]. [θ] in A is based on the molarity of the residue composed of a BINOL unit and a 27DIF unit.

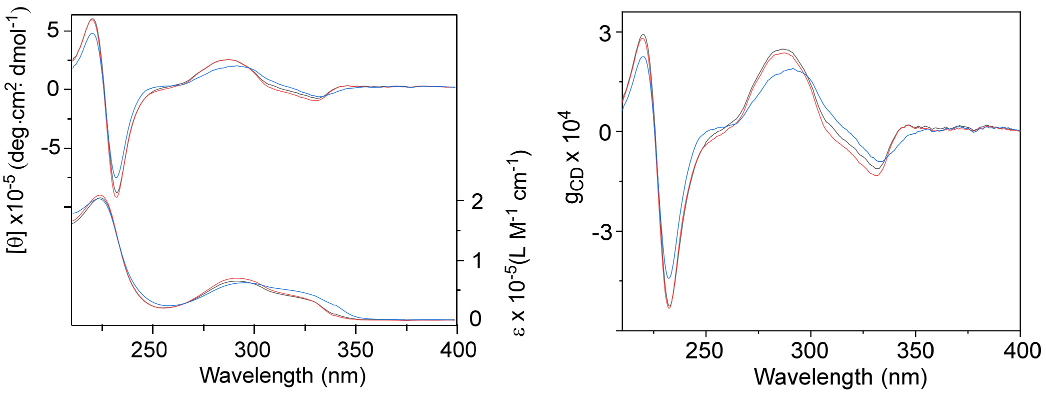

Fig. S9. CD-UV spectra of linear polymers obtained at 0 ºC (run 14 in Table S1) (a), 23 ºC (run 11 in Table S1) (b), and 50 ºC (run 15 in Table S1) (c) in THF [left] and corresponding g$_{CD}$ spectra [right]. [θ] in A is based on the molarity of the residue composed of a BINOL unit and a 27DIF unit.

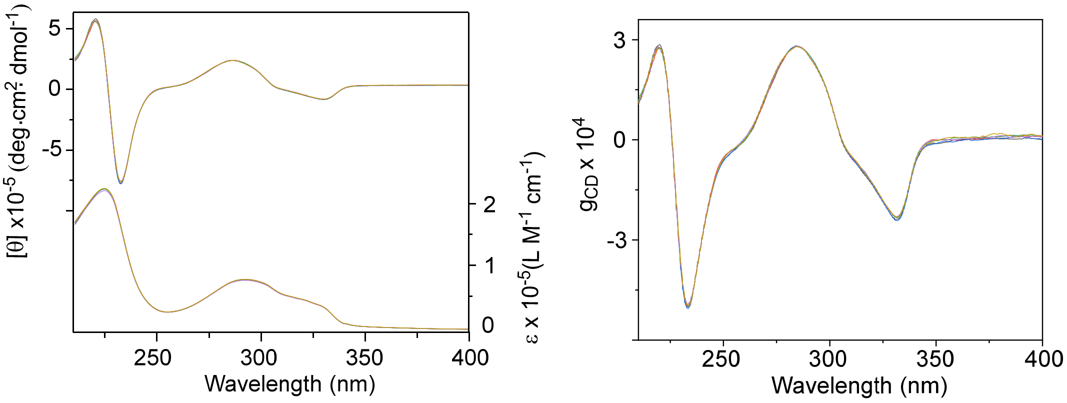

Fig. S10. CD-UV spectra of poly((R)-BINOL-alt-27DIF) in THF at 3.6 × 10^{-5} M (per residue) observed upon irradiation with an Hg-Xe lamp (5 mW) [left] and corresponding g$_{CD}$ spectra [right]. The sample was irradiated for a 1-min duration five times. [θ] is based on the molarity of the residue composed of a BINOL unit and a 27DIF unit.

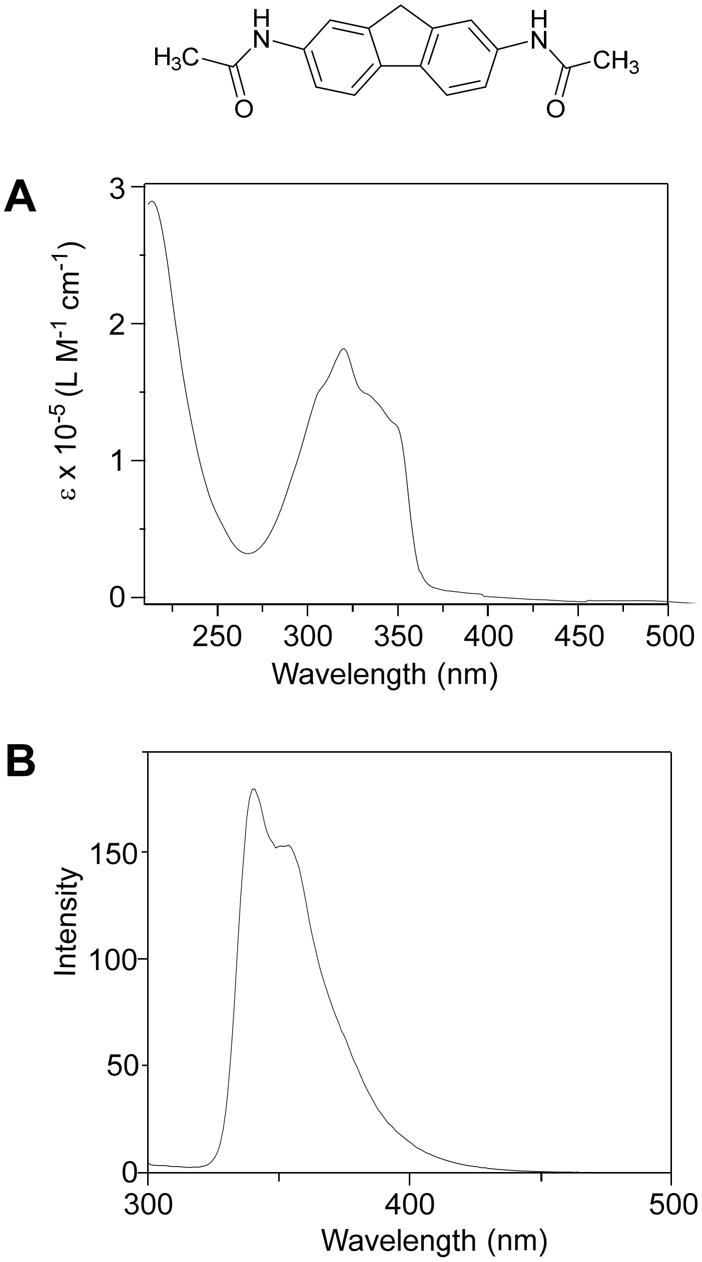

Fig. S11. Absorbance (A) and fluorescence (B) spectra of *N,N'*-(fluorene-2,7-diyl)diacetamide in THF. [conc. = 3.6 x 10^{-5} M (A), 7.1 x 10^{-6} M (B); λ_{ex} = 270 nm (B); cell path = 1 mm (A), 10 mm (B)]

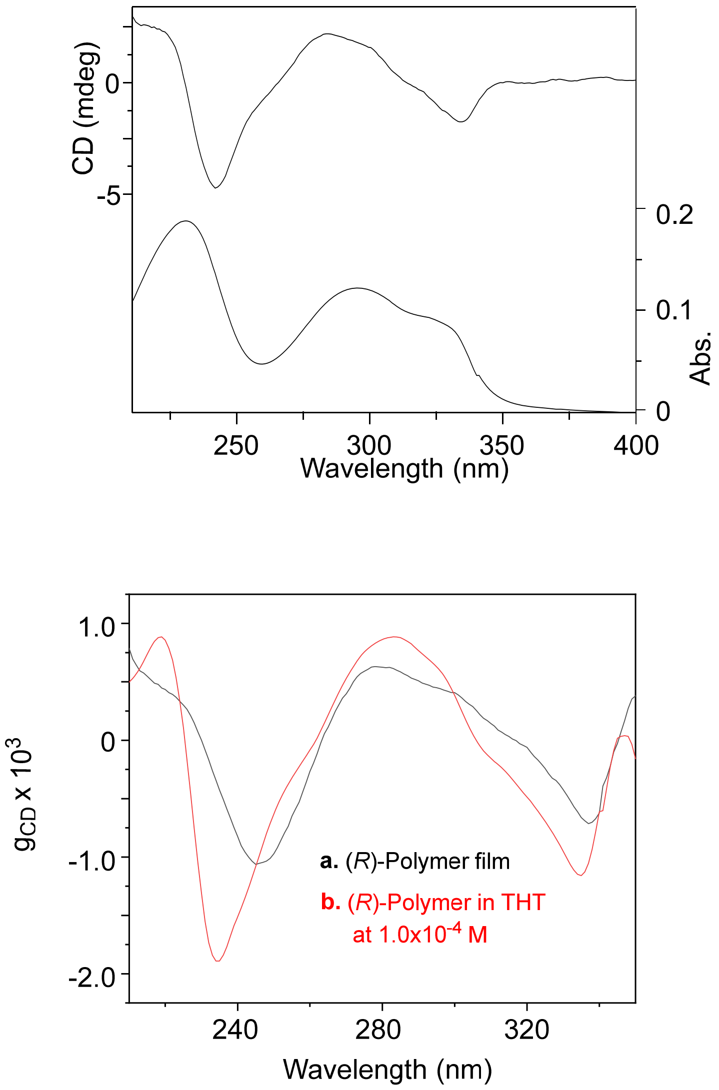

Fig. S12. CD-UV spectra of poly((*R*)-BINOL-*alt*-27DIF) [M_n 4100] in film formed on a quartz glass plate (top) and those of the same polymer in film and in solution (a = film, b = solution).

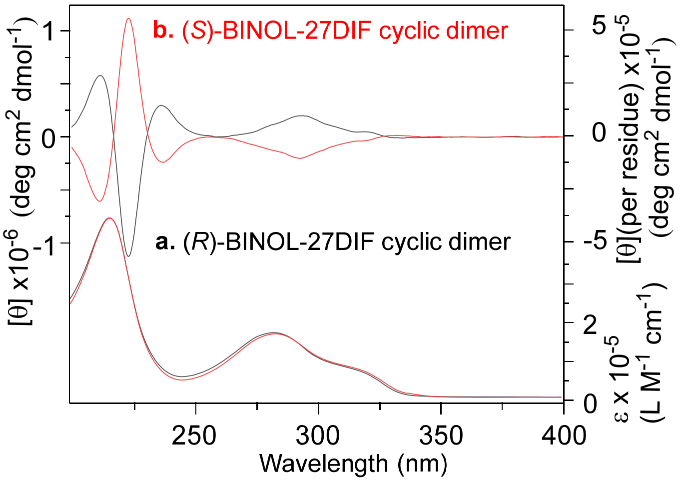

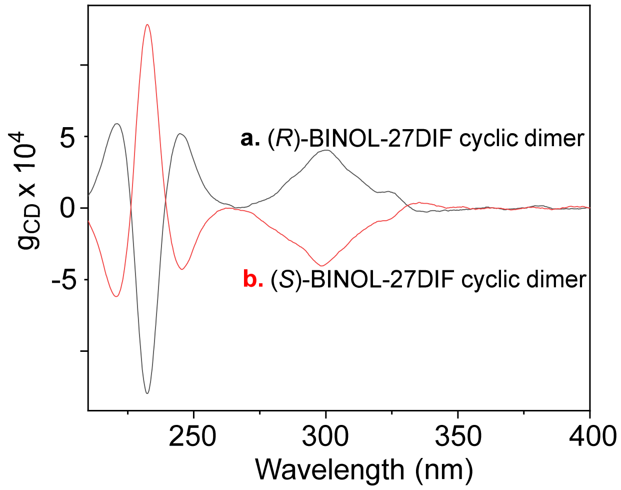

Fig. S13. CD-UV spectra of (*R*)-BINOL-27DIF cyclic dimer (a) and (*S*)-BINOL-27DIF cyclic dimer (b) [top] and corresponding g_{CD} spectra [bottom]. [θ]and $[\theta]_{\text{(per residue)}}$ in A are based on the molarity of cyclic dimer and that of the residue composed of a BINOL unit and a 27DIF unit, respectively. [Experimental spectral measurement conditions: THF, 1.1 x 10^{-4} M, 1-mm cell].

A. 1.0 x 10^{-4} M

Peak #1: Mean Diam. = 11.0 nm, S.Dev. = 0.7 nm (6.5%) Intens. = 73.7 %
Peak #2: Mean Diam. = 163.9 nm, S.Dev. = 18.5 nm (11.3%) Intens. = 26.3 %

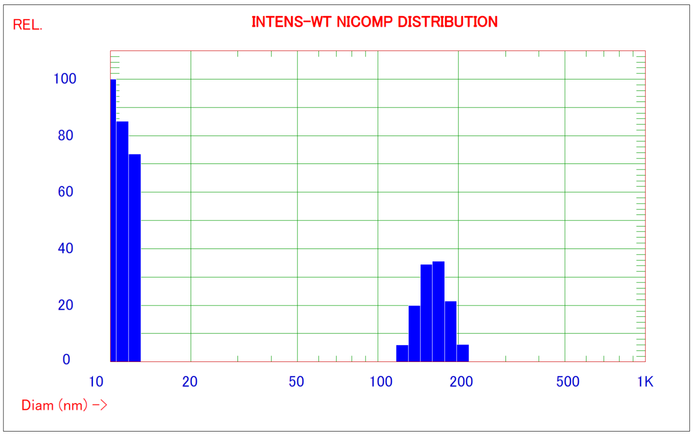

B. 1.0 x 10^{-6} M

Peak #1: Mean Diam. = 11.0 nm, S.Dev. = 0.7 nm (6.5%) Intens. = 100.0 %

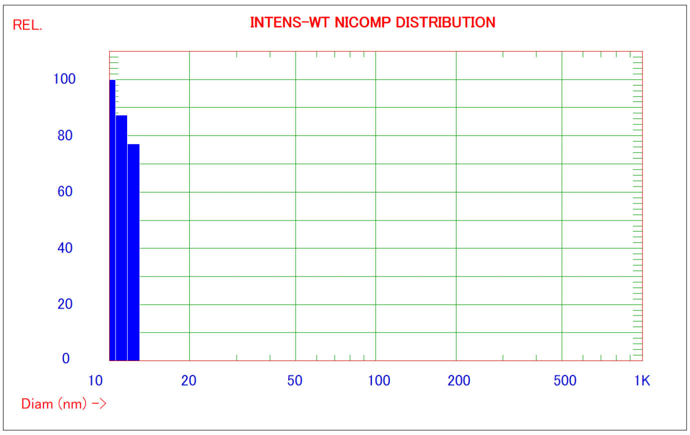

Fig. S14. DLS profiles of poly((*R*)-BINOL-alt-27DIF) observed at 1. 0 x 10^{-4} M (A) and 1. 0 x 10^{-6} M (B) in THF. [10-mm quartz cell]

Peak #1： Mean Diam. = 11. 1 nm, S. Dev. = 0. 7 nm （6. 4%） Intens. = 95. 4 %
Peak #2： Mean Diam. = 99. 0 nm, S. Dev. = 6. 5 nm （6. 6%） Intens. = 4. 6 %

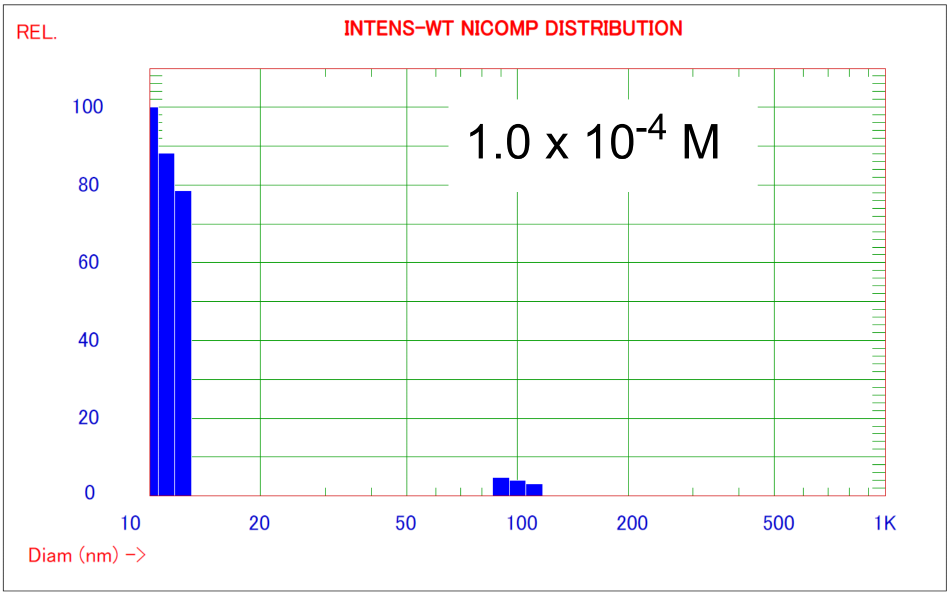

Peak #1： Mean Diam. = 12. 5 nm, S. Dev. = 1. 6 nm （13. 1%） Intens. = 100. 0 %

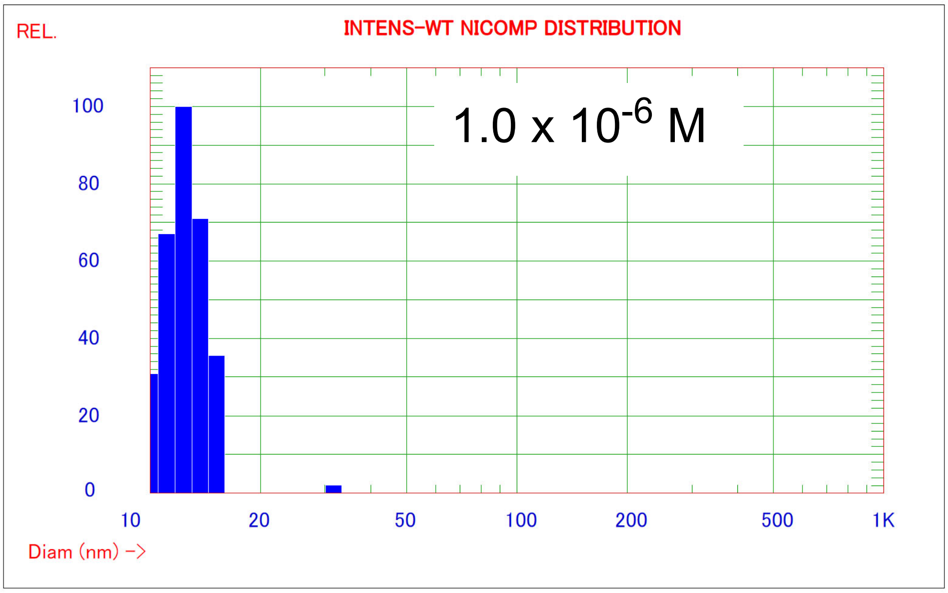

Fig. S15. DLS profiles of (*R*)-BINOL-27DIF cyclic dimer observed at 1. 0 x 10^{-4} M (A) and 1. 0 x 10^{-6} M (B) in THF. [10-mm quartz cell]

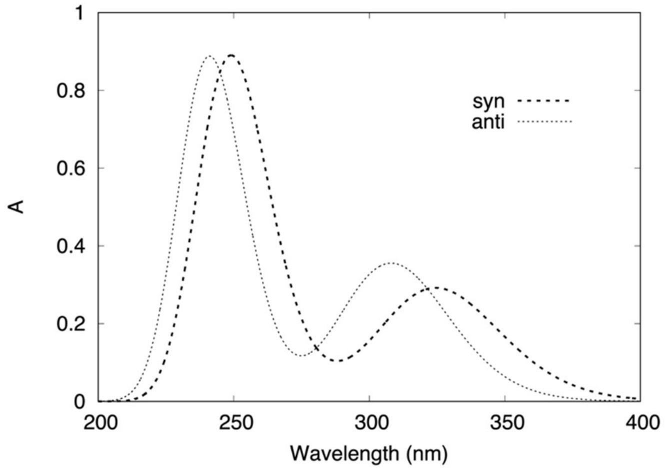

Fig. S16. Theoretical UV spectra of syn and anti conformers of (R)-BINOL-27DIF trimer.

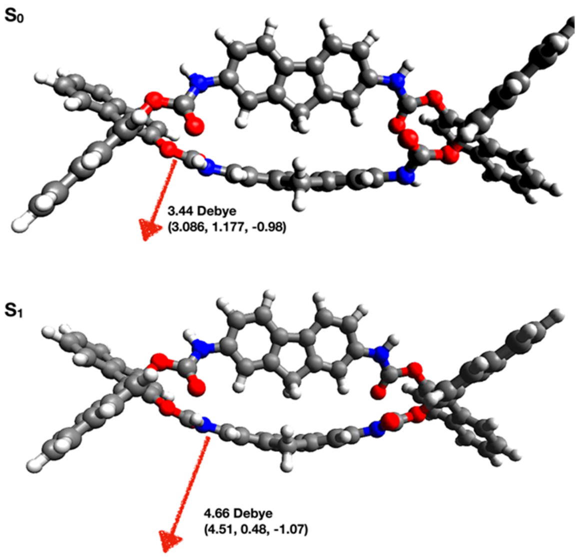

Fig. S17. Cyclic dimers structures optimized by DFT in the ground state (S_0) (top) and in the lowest excited state (S_1) (bottom) with red arrows depicting electric dipole moment vectors.

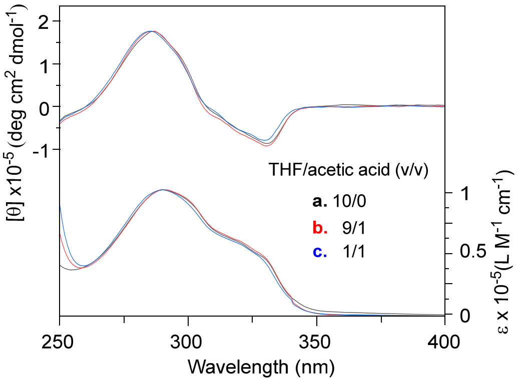

Fig. S18. CD-UV spectra of poly((*R*)-BINOL-*alt*-27DIF) in THF in the presence of acetic acid: [THF]/[acetic acid] = 10/0 (pure THF) (a), 9/1 (b), and 1/1 (c). [conc. 1.00 x 10^{-4} M, cell path = 1 mm]

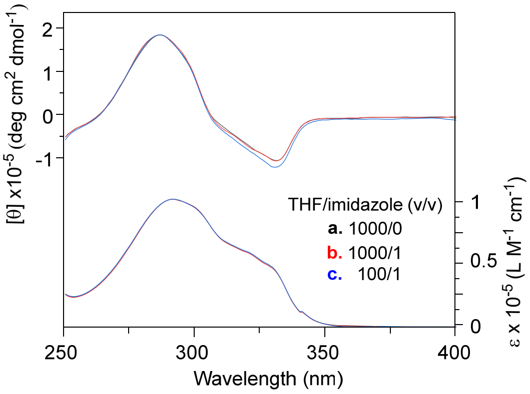

Fig. S19. CD-UV spectra of poly((*R*)-BINOL-*alt*-27DIF) in THF in the presence of imidazole: [THF]/[imidazole] = 1000/0 (pure THF) (a), 1000/1 (b), and 1000/10 (c). [conc. 1.00 x 10^{-4} M, cell path = 1 mm]

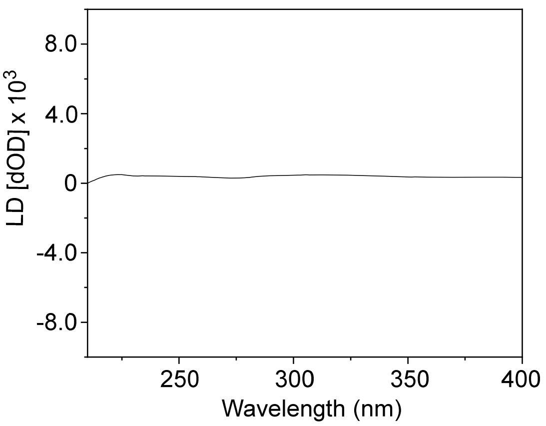

Fig. S20. LD spectrum of poly((*R*)-BINOL-*alt*-27DIF) in THF. [conc. 1.00 x 10^{-4} M, cell path = 1 mm]

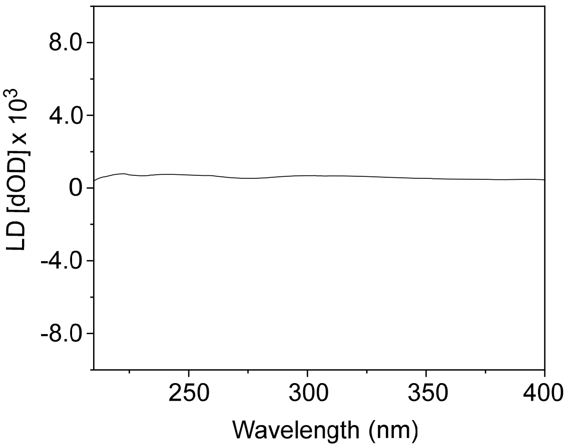

Fig. S21. LD spectrum of (*R*)-BINOL-27DIF cyclic dimer in THF. [conc. 1.00 x 10^{-4} M, cell path = 1 mm]

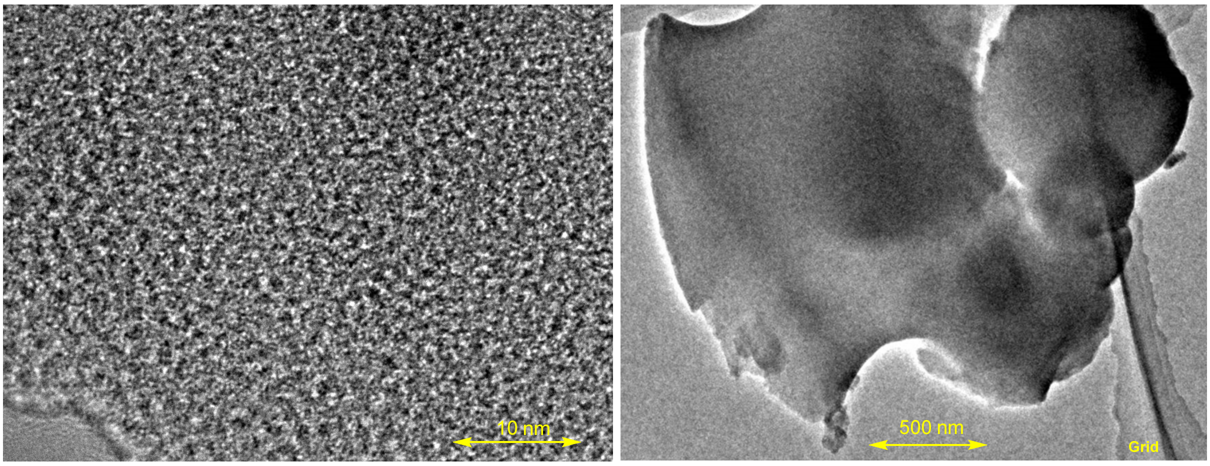

Fig. S22. TEM images of poly((*R*)-BINOL-*alt*-27DIF).

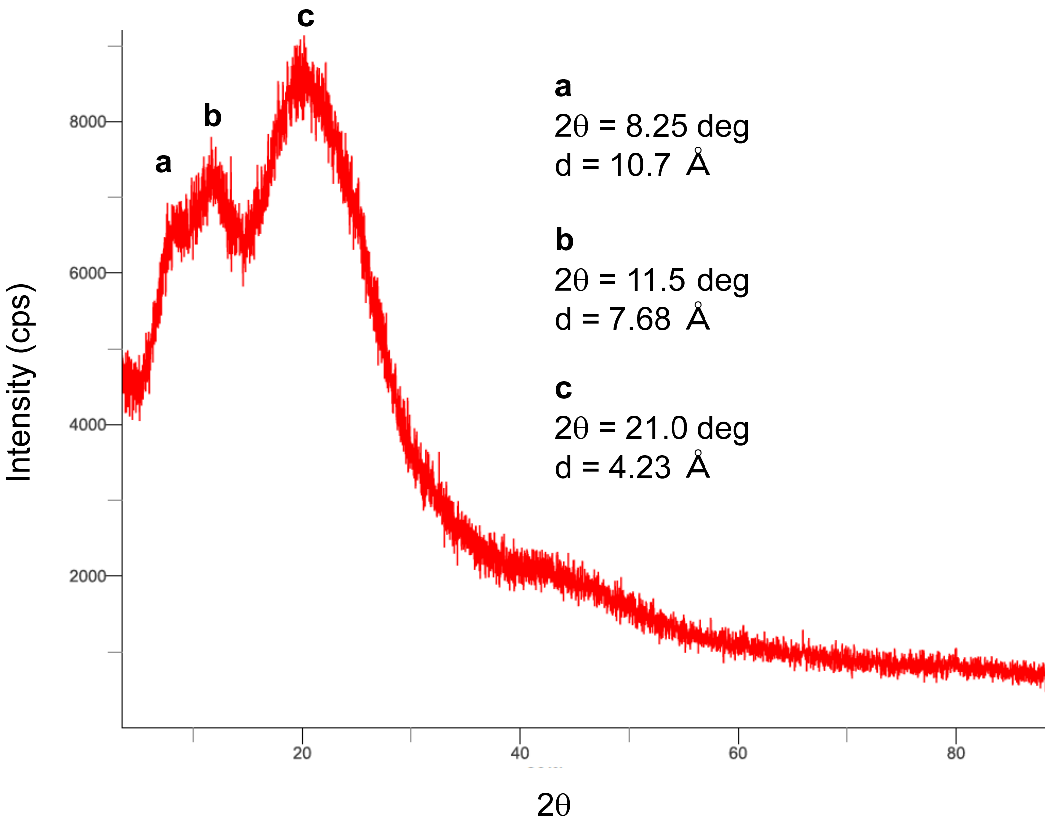

Fig. S23. XRD profile of poly((*R*)-BINOL-*alt*-27DIF).

References

1. S. Tanaka, K. Sato, K. Ichida, T. Abe, T. Tsubomura, T. Suzuki and K. Shinozaki, *Chem. Asian J.,* 2016, **11**, 265-273.
2. Y. Zhang, M. Tan, H. Li, Y. Zheng, S. Gao, H. Zhang and J. Y. Ying, *Chem. Commun.*, 2011, **47**, 7365-7367.
3. G. M. Sheldrick, *SHELXS-2013*, *A program for crystal structure determination*; University of Göttingen, Göttingen, Germany, 2013.
4. G. M. Sheldrick, *SHELXL-2014*, *A program for crystal structure refinement*; University of Göttingen, Göttingen, Germany, 2014.
5. H. Sun, *J. Phys. Chem. B*, 1998, **102**, 7338-7364.
6. R. Fletcher and C. M. Reeves, *Comput. J.*, 1964, **7**, 149-154.
7. H. J. C. Berendsen, J. P. M. Postma, W. F. van Gunsteren, A. DiNola and J. R. Haak, *J. Chem. Phys.*, 1984, **81**, 3684-3690.
8. S. S. Iyengar, H. B. Schlegel, J. M. Millam, G. A. Voth, G. E. Scuseria and M. J. Frisch*, J. Chem. Phys.*, 2001, **115**, 10291-302.
9. H. B. Schlegel, J. M. Millam, S. S. Iyengar, G. A. Voth, G. E. Scuseria, A. D. Daniels and M. J. Frisch, *J. Chem. Phys.*, 2001, **114**, 9758-63.
10. M. J. Frisch et al., Gaussian 16, Revision B.01, Gaussian, Inc.: Wallingford, CT, 2016.
11. J. Ridley and M.C. Zerner, *Theor. Chim. Acta*, 1973, **32**,111-134.
12. J. Ridley and M.C. Zerner, *J. Mol. Spectrosc.,* 1974, **50**, 457-473.
13. F. Furche, R. Ahlrichs, C. Wachsmann, E. Weber, A. Sobanski, F. Voegtle and S. Grimme, *J. Am. Chem. Soc.*, 2000, **122**, 1717-1724.
14. N. Sreerama and R. Woody, *Methods Enzymol.*, 2004, **383**, 318-351.
15. A. Koslowski, N. Sreerama, R. W. Woody, Theoretical Approach to Electronic Optical Activity. In Circular Dichroism – Principles and Applications; Berova, N., Nakanishi, K., Woody, R. W., Eds.; *Wiley-VCH: New York*, 2000; pp 55–95.
16. S. Grimme, *Rev. Comput. Chem,* 2004, **20**, 153-218.
17. J. D. Chai M. Head-Gordon, *Phys. Chem. Chem. Phys.*, 2008, **10**, 6615-6620.
18. B. H. Besler, K. M. Merz Jr and P. A. Kollman, *J. Comp. Chem.*, 1990, **11**, 431-439.